2022 IEEE Microwaves, Antennas, and Propagation Conference (MAPCON) | 978-1-6654-5203-8/22/$31.00 ©2022 IEEE | DOI: 10.1109/MAPCON56011.2022.10047705

Dual-Band Substrate Integrated Waveguide (SIW) Cavity Slot Antenna for C-Band Applications

Anil Kumar Nayak[1,2], Meenal Chouhan[1], Kambiz Moez[2], M. V. Kartikeyan[3], Amalendu Patnaik[1]
Dept. of Electronics and Communication Engineering[1], Dept. of Electrical and Computer Engineering[2,3]
Indian Institute of Technology Roorkee[1], University of Alberta[2], Indian Institute Of Technology Tirupati[3]
Roorkee, Uttarakhand, India[1], Edmonton Canada[2], Triupati, Andra Pradesh, India[3]
Email: anayak@ec.iitr.ac.in

***Abstract*—This paper presents a dual-band substrate integrated waveguide (SIW) cavity slot antenna with improved performance in terms of impedance matching, radiation efficiency, gain, and reduced cross-polarization level for C-band application. A pair of diagonal corner truncated L-shape slots on the SIW cavity generates circular polarization (CP) and linear polarization (LP). Two shorting pins are placed near a feed line to realize better impedance matching. A square patch antenna with truncated corners is designed on a SIW for circular polarization, and two shorting pins are used near the feed line for better impedance matching. The radiation pattern of the proposed antenna is LP at 5.43 GHz and CP at 5.98 GHz. The impedance bandwidth for reflection coefficient below -10 dB is between 5.35 to 5.55 GHz and 5.85-6.05 GHz for the lower and the upper band, respectively. In addition, a 3-dB axial ratio bandwidth of 0.375 GHz is observed at the upper band owing to the CP radiation. The measured peak realized gains of the LP mode and the CP mode are 8.13 dBi and 8.9 dBic. The radiation efficiencies at the lower and upper bands are above 89% and 88%, respectively. The measured results are in good agreement with the simulation data.**

***Index Terms*—Circular polarization (CP), impedance matching, linear polarization (LP), substrate integrated waveguide (SIW), radiation efficiency.**

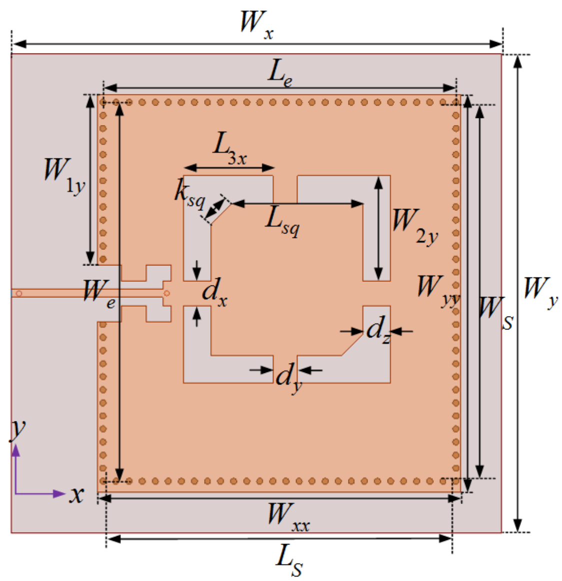

Fig. 1. Top view of the proposed antenna structure.

I. Introduction

Due to the increased use of radio frequency (RF) and microwave for the communication systems, planar antennas with various radiating elements, feeding structures, and different polarization have received significant attention from researchers around the globe. Circularly polarized (CP) antennas are widespread because of their ability to avoid contrary effects caused by Faraday rotation, multipath reflections, and polarization incongruity due to misalignments between transmitter and receiver antennas. The primary advantages of CP antennas are: (1) steady signal strength between the transmitter and receiver; (2) easier installation regardless of the antenna's orientation; (3) ease of fabrication; and (4) it counters the impact of weather dispersion compared to the linearly polarized (LP) antennas. [1], [2]. To improve the CP antenna's performance, several techniques for the generation of CP waves have been reported in [3]–[10]. Different concepts and techniques have been documented to obtain CP, by using microstrip patch and SIW, etc. These techniques include elliptical patch, square patch, circular patch with perturbations, circular patch with slot, and square patch with slot [11]. The SIW-based linearly polarized antennas are reported in [12], [13]. Similarly, single-band and dual-band CP SIW antennas are proposed in [14]–[21]. The CP antennas in [16] and [17], have the same sense of polarization in both bands.

This paper aims to improve performance parameters in a single layer, dual-bandSIW cavity slot antenna structure radiating waves of two different polarizations. Initially, a microstrip patch antenna is designed for dual-band operation. This antenna structure is made to resonate in two bands by placing a shorting pin at the end of the feed. It gives better impedance matching between the antenna and feed. In order to

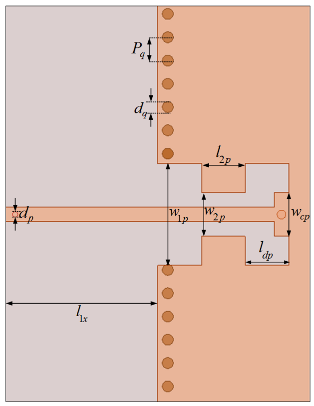

Fig. 2. Enlarged view of feed line of the proposed antenna.

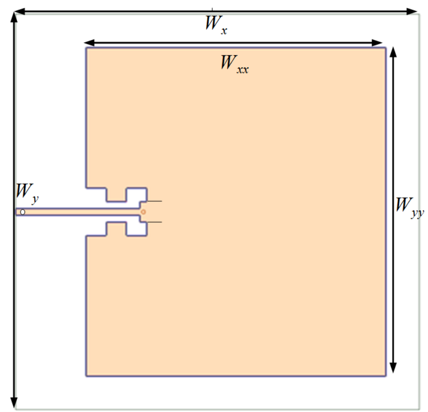

Fig. 3. Top view of patch antenna.

obtain the low cross-polarization level and lateral leakage loss, the SIW is implemented in the proposed antenna. Additionally, the design places a slot and square patch with corners truncated to achieve the enhanced antenna performance along with the circular polarization. As a result, the proposed antenna has a low cross-polarization level, high front-to-back ratio (FTBR), improved gain, efficiency, and compact size.

II. Antenna Structure Design and Analysis

The top view of the proposed antenna is shown in Fig. 1 and its corresponding enlarged view feed section in Fig. 2. The dielectric substrate used for the proposed antenna is Rogers $RO4232^{(TM)}$ (ϵ_r = 3.2, tan, δ = 0.0018, according to data sheet) of thickness 1.524 mm. The simulation results presented in this paper are obtained by performing full-wave analysis in Ansys HFSS ver. 2020R2, and are verified experimentally.

A. Dual-Band Microstrip Patch Antenna

The top view of the microstrip patch antenna is depicted in Fig. 3. Initially, the antenna is designed for C-band frequency. The antenna dimensions are calculated at the same frequency range (C-band). In order to fix the diameter of shorting pin, an optimization method is adopted in this proposed work. This method uses notches inside the patch conductor nearby the shorting pin and yields an additional reduction in the conductor dimension. Near the feed section, rectangular shorted patches have been implemented, and the finding can be applied to any other form of the shorted patch. Two notches have been interpreted as three conductor pads (see Fig. 2). The first pad is located near the short circuit, and the second and third are in front of the feed. The impedance performance is affected because of the dimensions of each pad. The length of the first padl_{2p} should be fixed to keep the radius of the shorting pin and achieve the reduced patch size. The width of the first pad W_{cp} plays a crucial role in affecting the antenna size and improving the input impedance. If the width of the feed is equal to the W_{cp}, then the antenna acts as a short patch. As the dimension of W_{cp} is reduced, the overall dimension of the patch decreases due to fringing capacitance. The maximum reduction is achieved when the radius of shorting pin is reduced. The width of the first pad is decreased. In this case, the input impedance is reduced, and the antenna looks the same as a short circuit at a feed point. Using the parametric variation to fix the dimension between maximum size reduction and required input impedance behavior. This change of the input impedance leads to improving the required and accurate putting of the shorting pin with respect to the feed of a standard shorted patch.

The existence of the other two pads again increases the fringing capacitance created around the feed or post, leading to a reduction in the size of the conductor. These extra pads have provided an effect on the impedance behavior. Finally, the first and second resonance frequencies are obtained for two respective notches of the patch.

B. Dual-Band SIW Cavity Slot Antenna

The SIW based planar antennas are preferred not only in microwave regions but also for millimeter antennas because of the high-power handling capability, compact, lighter weight, and low loss. Proper and suitable design of SIW leads to negligible radiation loss compared to microstrip patch antenna. It also increases the efficiency of planar antenna structures and helps in decreasing the cross-polarization level. The design process of a microstrip antenna using SIW consists of three-steps, First implementing the dimensions of SIW, the pitch P_q and via diameter d_q have been calculated as mentioned in [22]:

$$d_q \leq \frac{\lambda_g}{5},\ \lambda_g = \frac{\lambda_o}{\sqrt{\varepsilon_e}},\ and\ P_q \leq 2d_q \tag{1}$$

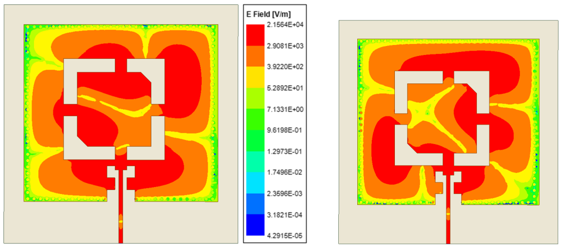

(a) (b)

Fig. 4. Electric field distribution and different eigen mode of the SIW cavity: (a) TE_{201} and (b) TE_{202}.

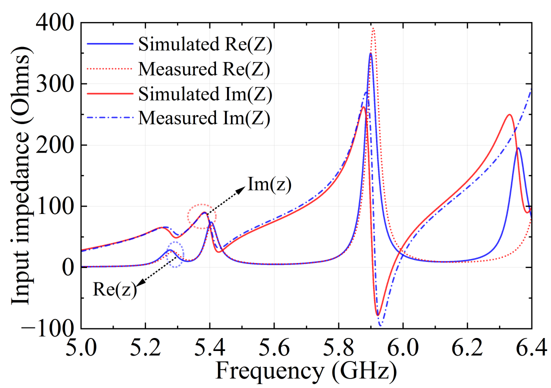

Fig. 5. Simulated input impedance vs frequency plot.

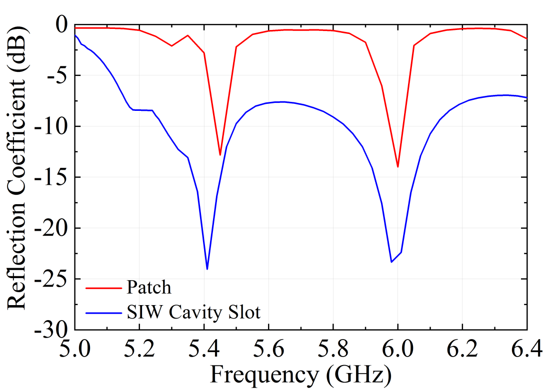

Fig. 6. Simulated reflection coefficient patch and SIW cavity slot antenna.

where λ_g and λ_0 are the guided wavelength and wavelength in free space. Whereas the ε_e is the effective dielectric constant of the medium:

$$\frac{d_q}{P_q} \geq \frac{1}{2} \; and \; \frac{d}{\lambda_0} \leq \frac{1}{10} \tag{2}$$

here λ_c is the cutoff wavelength. The resonant frequency of the TE_{mnp} mode of the rectangular SIW resonator can be determined according to the following formulas:

$$f_{mnp(r))} = \frac{c}{2\sqrt{\varepsilon_r}} \sqrt{\left(\frac{m}{L_e}\right)^2 + \left(\frac{n}{h}\right)^2 + \left(\frac{p}{W_e}\right)^2} \tag{3}$$

Thus, the resonant frequency of TE_{201} and $TE_{202}-$modes can be calculated based on the values of m, n, p corresponding to a specific dimensions as mentioned in Fig. 1 and 2, as shown in Fig. 4:

$$f_{201} = \frac{c}{2\sqrt{\varepsilon_r}} \sqrt{\left(\frac{2}{L_e}\right)^2 + \left(\frac{1}{W_e}\right)^2} \tag{4}$$

$$f_{202} = \frac{c}{2\sqrt{\varepsilon_r}} \sqrt{\left(\frac{2}{L_e}\right)^2 + \left(\frac{2}{W_e}\right)^2} \tag{5}$$

$$\begin{cases} L_e = L_S - 1.08\frac{d_q^2}{P_q} + 0.1\frac{d_q^2}{L_S} \\ W_e = L_S - 1.08\frac{d_q^2}{P_q} + 0.1\frac{d_q^2}{L_S} \end{cases} \tag{6}$$

where $m = 1, 2, 3, \cdots\cdot$, $n = 1, 2, 3, \cdots\cdot$, and $p = 1, 2, 3, \cdots\cdot$. Finally, the theoretically resonant frequencies are 4.9 GHz and 6.06 GHz at TE_{201} and TE_{202} eigen modes, respectively. The structure dimensions are $W_{1y} = 19.87$, $W_x = 58$, $W_y = 56.75$, $W_{xx} = 42.55$, $W_{yy} = 46.85$, $P_q = 1.6$, $d_q = 0.8$ $d_p = 1$, $w_{1p} = 7$, $w_{2p} = 3$, $l_{2p} = 3$, $l_{dp} = 3$, $l_{1x} = 13$, $d_x = 0.8$, $d_y = 3$, $d_z = 3$, $W_{2y} = 11$, $L_{3x} = 9.5$, $w_{cp} = 3$, $k_{sq} = 3.96$, $w_{sp} = 2$, $W_S = 40.9$, $L_S = 38.2$, $W_e = 40.52$, $L_e = 37.82$, $h = 1.524$; unit: millimeters (see Fig. 1 and 2).

One of the most important characteristics of the proposed antenna design is the impedance matching. In view of this, input impedance study was carried out and is plotted in Fig. 5. For perfect matching the input impedance looking into the microstrip feedline must be close to the characteristic impedance of the line. The real part of the input impedance at the desired frequency is around 50 Ω and simultaneously the imaginary part is approximately zero. Henceforth, as shown in Fig. 6, the return loss is found to be minimum in microstrip patch antenna and the better impedance matching with the SIW cavity slot antenna at the corresponding resonance frequencies.

Due to the SIW implementation in the patch, it behaves like a cavity resonator. Furthermore, by putting four symmetrically L-type slots in this design. This structure act as an SIW cavity slot antenna. However, the antenna propagates only the linear polarization. In order to obtain a circular polarization, two corners of the square patch are truncated in the antenna. Fig. 7 illustrate the surface current distribution at 5.98 GHz. It can be observed from plots, the direction of suface current is changed in every 90^0 phase (($\omega t = 0^0$, 90^0, 180^0, and 270^0)), as shown in Fig. 7 (a)-(d). As a result, the nature of polarization is left

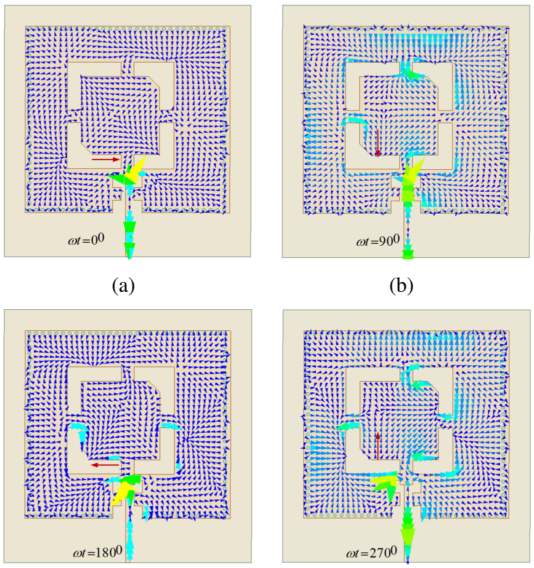

(a) (b) (c) (d)

Fig. 7. Surface current distribution (vector) at 5.99 GHz: (a) $\omega t = 0$ (b) $\omega t = \frac{\pi}{2}$ (c) $\omega t = \pi$ (d) $\omega t = \frac{3\pi}{2}$.

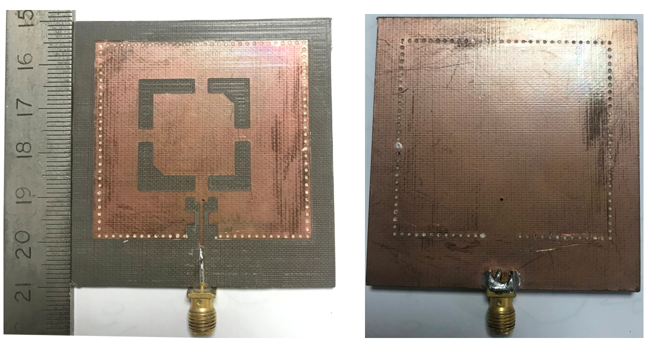

(a) (b)

Fig. 8. Fabricated prototype of proposed antenna: (a) Top view and (b) bottom view.

hand circular polarization (LHCP). In contrast, the first band propagated is linearly polarized (LP). Furthermore, the sorting pin diameter is fixed at d_p = 1 mm by the parametric variation method and the slot width d_y=3 mm.

III. Fabrication, Measurements and Discussion

The top and bottom view of the fabricated prototype of SIW cavity slot antenna is shown in Fig. 8. In order to maintain loss-free radiation of the proposed structure, the fabrication and filling of the copper paste into the vias are done carefully. The measured and simulation results of the reflection coefficient SIW cavity slot antenna is shown in Fig. 9. It can be observed that the frequency slightly shifts because of the manual fill

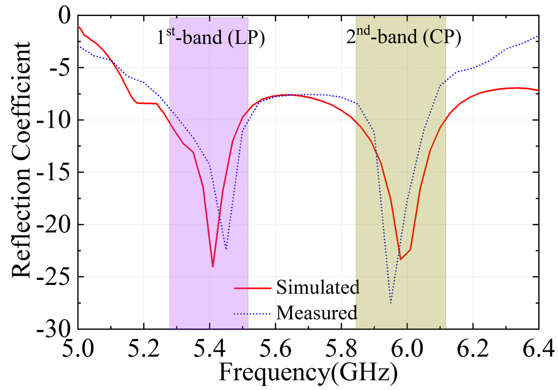

Fig. 9. Simulated and measured reflection coefficient.

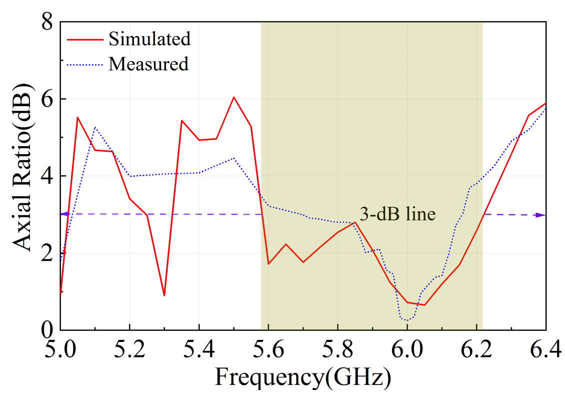

Fig. 10. Simulated and measured axial ratio of the proposed antenna.

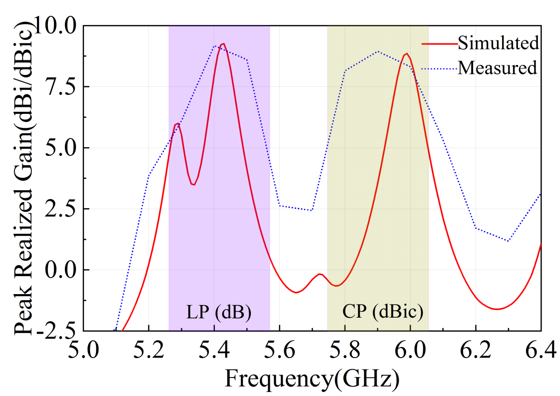

Fig. 11. Simulated and measured peak realized gain vs frequency

Table I
COMPARISON OF VARIOUS DUAL-BAND SIW ANTENNAS

Ref.	Resonant Frequency (GHz)		Size (λ_0^2)		Polarization	Max. Gain LP (dBi) and CP (dBic)	Impedance Bandwidth (%)	Efficiency (%)
	f_1	f_2	f_1	f_2				
[18]	12.5	13.625	0.99×0.99	1.08×1.08	CP	2.2 and 4.7	16	96 and 98
[19]	10	10.7	2.16×1.136	2.31×1.46	LP	8.14	8.5	75
[20]	10	12	1.34×1.867	1.6×2.24	LP	8.5	7.3 and 7.76	87
[21]	37.5	47.8	1×1.275	1.274×1.625	CP	5 and 5.7	1.1 and 1.4	88 and 93
This work	5.42	5.98	0.76×0.93	0.77×0.85	LP and CP	8.13 and 8.9	3.74 and 3.35	89 and 88

f_1: lower resonant frequency; f_2: higher resonant frequency

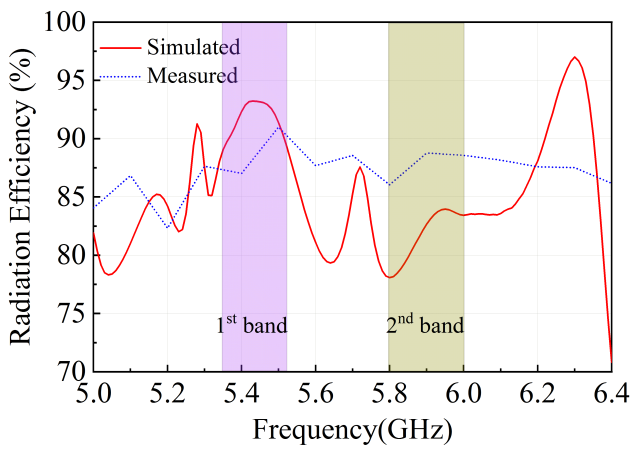

Fig. 12. Simulated and experimental plot of radiation efficiency.

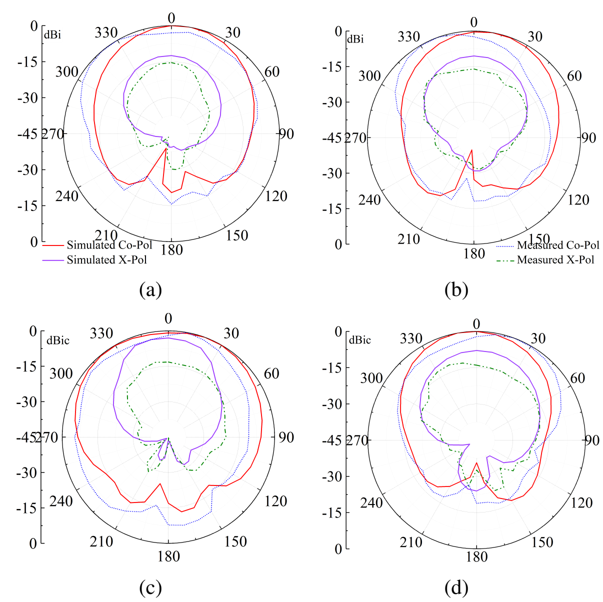

Fig. 13. Simulated and experimental normalized radiation pattern: (a) E-plane, (b) H-plane at f_1 frequency, and (c) E-plane, (d) H-plane at f_2.

of metallic paste into the vias, SMA connector and conductor loss. As shown in Fig. 9, the measured return loss is less than 10 dB from 5.35 to 5.55 GHz and 5.85 to 6.05 GHz. The fractional impedance bandwidths range from 5.35 to 5.55 GHz and 5.85 to 6.05 GHz are 3.70% and 3.35%, respectively. The measured and simulation results of the axial ratio of the proposed antenna are plotted, as illustrated in Fig. 10. The 3-dB axial ratio bandwidth of 0.375 GHz is achieved.

The simulated and experimental results of the peak realized gain of the SIW cavity slot antenna are shown in Fig. 11. The measured gain is the same as the simulated data of the proposed antenna. However, it is slightly less because resonant frequency is shifted up for lower resonant frequency and downward for higher resonant frequency. The experimental value of peak realized gain of 8.13 dBi and 8.9 dBic (simulated: 8.24 dBi and 9.12 dBic) are obtained at the lower and higher resonant frequencies, respectively.

By using Wheeler cap method, the reflection coefficient is measured in the free space. Then, the antenna is enclosed by a conductor. At this condition, the reflected power is returned to the feeding port. The radiated power is measured by comparing the reflection coefficient in the free space [20].

$$\eta_{meas} = 1 - \frac{P_{loss}}{P_{in}} = 1 - \frac{1-|\Gamma_{wc}|^2}{1-|\Gamma_{fc}|^2} = \frac{|\Gamma_{wc}|^2 - |\Gamma_{fc}|^2}{1-|\Gamma_{fc}|^2} \quad (7)$$

Where η_{meas} is the measured radiation efficiency, $|\Gamma_{wc}|$ is the magnitude of the reflection coefficient using Wheeler cap method and $|\Gamma_{fc}|$ is the magnitude of the reflection coefficient in free space. The simulated and measured results of radiation efficiency of the SIW cavity slot antenna is shown in Fig.12. Although measured results are slightly lesser than the simulated results of SIW based slot antenna, these two curves are in good agreement with each other at the corresponding resonant frequency. The measured radiation efficiencies of 89%, and 88% (simulated: 93% and 87%,) are found at the corresponding resonant frequencies, respectively as shown in Fig. 12.

The radiation pattern of E-plane and H-plane at 5.42 and 5.98 GHz are observed and shown in Fig.13. The cross polarization is lower than the co-polarization in both measured and simulated results. The cross-polarization is -15 to -25 dB lower than the normalized radiation pattern, because SIW reduces cross-polarization and has negligible leakage loss. The measured results are in good agreement with simulation results and the same has been verified all the above plots.

In Table I, the performance of previous dual band antennas [18]–[21], is compared with the present work. It should be noted that the previously reported dual band SIW antennas have the same polarization as the bands whereas the proposed antenna can provide different polarization at the different bands. The size of the proposed antenna in terms of free space wavelength is lesser than in [18]–[21]. It can be observed that the peak realized gain is higher than in [18]–[21]. The radiation efficiency is higher than in [19] and [20] and impedance bandwidth is slightly higher than in [21].

IV. Conclusion

In this paper, a dual band SIW cavity slot antenna with improved performance has been presented. The proposed antenna is fed by the feeding network consisting of two notches, operates at two different frequencies and with two different polarizations. The proposed antenna operates at two bands (5.35-5.55 GHz, and 5.85-6.05 GHz) with gain of 8.13 dBi, and 8.9 dBic respectively and one CP bandwidth is obtained from 5.77 to 6.15 GHz (FBW: 6.27%) at 3-dB axial ratio. The measured results are in good agreement with simulated result for designed antenna. This antenna can be used for C-band applications.

References

[1] J.-Y. Sze, C.-I. G. Hsu, Z.-W. Chen, and C.-C. Chang, "Broadband cpw-fed circularly polarized square slot antenna with lightening-shaped feedline and inverted-l grounded strips," *IEEE Transactions on Antennas and Propagation*, vol. 58, no. 3, pp. 973–977, 2010.

[2] R. K. Saini and S. Dwari, "A broadband dual circularly polarized square slot antenna," *IEEE Transactions on Antennas and Propagation*, vol. 64, no. 1, pp. 290–294, 2016.

[3] T.-N. Chang, "Wideband circularly polarised antenna using two linked annular slots," *Electronics Letters*, vol. 47, pp. 737–739(2), June 2011.

[4] J. Pourahmadazar, C. Ghobadi, J. Nourinia, N. Felegari, and H. Shirzad, "Broadband cpw-fed circularly polarized square slot antenna with inverted-l strips for uwb applications," *IEEE Antennas and Wireless Propagation Letters*, vol. 10, pp. 369–372, 2011.

[5] N. Felegari, J. Nourinia, C. Ghobadi, and J. Pourahmadazar, "Broadband cpw-fed circularly polarized square slot antenna with three inverted-l-shape grounded strips," *IEEE Antennas and Wireless Propagation Letters*, vol. 10, pp. 274–277, 2011.

[6] J. N. M. O. Gh. Beigmohammadi, Ch. Ghobadi, "Small square slot antenna with circular polarisation characteristics for wlan/wimax applications," *Electronics Letters*, vol. 46, pp. 672–673(1), May 2010.

[7] T. Nakamura and T. Fukusako, "Broadband design of circularly polarized microstrip patch antenna using artificial ground structure with rectangular unit cells," *IEEE Transactions on Antennas and Propagation*, vol. 59, no. 6, pp. 2103–2110, 2011.

[8] G. T. T.N. Chang, "A wideband coplanar waveguide-fed circularly polarised antenna," *IET Microwaves Antennas & Propagation*, vol. 2, pp. 343–347, June 2008.

[9] A. K. Nayak and A. Patnaik, "Slw-based patch antenna with improved performance," in *2017 IEEE Applied Electromagnetics Conference (AEMC)*, 2017, pp. 1–2.

[10] W.-H. Tu and K. Chang, "Wide-band microstrip-to-coplanar stripline/slotline transitions," *IEEE Transactions on Microwave Theory and Techniques*, vol. 54, no. 3, pp. 1084–1089, 2006.

[11] K. W. Leung and H. K. Ng, "Theory and experiment of circularly polarized dielectric resonator antenna with a parasitic patch," *IEEE Transactions on Antennas and Propagation*, vol. 51, no. 3, pp. 405–412, 2003.

[12] R. Chair, S. Yang, A. Kishk, K. F. Lee, and K. M. Luk, "Aperture fed wideband circularly polarized rectangular stair shaped dielectric resonator antenna," *IEEE Transactions on Antennas and Propagation*, vol. 54, no. 4, pp. 1350–1352, 2006.

[13] G. Q. Luo, Z. F. Hu, Y. Liang, L. Y. Yu, and L. L. Sun, "Development of low profile cavity backed crossed slot antennas for planar integration," *IEEE Transactions on Antennas and Propagation*, vol. 57, no. 10, pp. 2972–2979, 2009.

[14] T. Zhang, W. Hong, Y. Zhang, and K. Wu, "Design and analysis of siw cavity backed dual-band antennas with a dual-mode triangular-ring slot," *IEEE Transactions on Antennas and Propagation*, vol. 62, no. 10, pp. 5007–5016, 2014.

[15] Q. Wu, J. Yin, C. Yu, H. Wang, and W. Hong, "Low-profile millimeter-wave siw cavity-backed dual-band circularly polarized antenna," *IEEE Transactions on Antennas and Propagation*, vol. 65, no. 12, pp. 7310–7315, 2017.

[16] F. Xu and K. Wu, "Guided-wave and leakage characteristics of substrate integrated waveguide," *IEEE Transactions on Microwave Theory and Techniques*, vol. 53, no. 1, pp. 66–73, 2005.

[17] H. Wang, D.-G. Fang, B. Zhang, and W.-Q. Che, "Dielectric loaded substrate integrated waveguide (siw) H-plane horn antennas," *IEEE Transactions on Antennas and Propagation*, vol. 58, no. 3, pp. 640–647, 2010.

[18] K. Kumar, S. Dwari, and M. K. Mandal, "Broadband dual circularly polarized substrate integrated waveguide antenna," *IEEE Antennas and Wireless Propagation Letters*, vol. 16, pp. 2971–2974, 2017.

[19] M. Mbaye, J. Hautcoeur, L. Talbi, and K. Hettak, "Bandwidth broadening of dual-slot antenna using substrate integrated waveguide (siw)," *IEEE Antennas and Wireless Propagation Letters*, vol. 12, pp. 1169–1171, 2013.

[20] L. Sabri, N. Amiri, and K. Forooraghi, "Dual-band and dual-polarized siw-fed microstrip patch antenna," *IEEE Antennas and Wireless Propagation Letters*, vol. 13, pp. 1605–1608, 2014.

[21] Q. Wu, J. Yin, C. Yu, H. Wang, and W. Hong, "Low-profile millimeter-wave siw cavity-backed dual-band circularly polarized antenna," *IEEE Transactions on Antennas and Propagation*, vol. 65, no. 12, pp. 7310–7315, 2017.

[22] J.-D. Zhang, L. Zhu, Q.-S. Wu, N.-W. Liu, and W. Wu, "A compact microstrip-fed patch antenna with enhanced bandwidth and harmonic suppression," *IEEE Transactions on Antennas and Propagation*, vol. 64, no. 12, pp. 5030–5037, 2016.